The Plant Cell, Vol. 23: 1435–1448, April 2011, www.plantcell.org

The *Arabidopsis thaliana* Checkpoint Kinase WEE1 Protects against Premature Vascular Differentiation during Replication Stress [W]

Toon Cools,[a,b] Anelia Iantcheva,[a,b,1] Annika K. Weimer,[c] Shannah Boens,[a,b] Naoki Takahashi,[a,b,2] Sara Maes,[a,b] Hilde Van den Daele,[a,b] Gert Van Isterdael,[a,b] Arp Schnittger,[c] and Lieven De Veylder[a,b,3]

[a] Department of Plant Systems Biology, VIB, 9052 Ghent, Belgium
[b] Department of Plant Biotechnology and Genetics, Ghent University, B-9052 Ghent, Belgium
[c] Department of Molecular Mechanisms of Phenotypic Plasticity, Institut de Biologie Moléculaire des Plantes–Centre National de Recherche Scientifique, Unité Propre de Recherche 2357, Université de Strasbourg, 67084 Strasbourg Cedex, France

A sessile lifestyle forces plants to respond promptly to factors that affect their genomic integrity. Therefore, plants have developed checkpoint mechanisms to arrest cell cycle progression upon the occurrence of DNA stress, allowing the DNA to be repaired before onset of division. Previously, the WEE1 kinase had been demonstrated to be essential for delaying progression through the cell cycle in the presence of replication-inhibitory drugs, such as hydroxyurea. To understand the severe growth arrest of *WEE1*-deficient plants treated with hydroxyurea, a transcriptomics analysis was performed, indicating prolonged S-phase duration. A role for WEE1 during S phase was substantiated by its specific accumulation in replicating nuclei that suffered from DNA stress. Besides an extended replication phase, *WEE1* knockout plants accumulated dead cells that were associated with premature vascular differentiation. Correspondingly, plants without functional *WEE1* ectopically expressed the vascular differentiation marker *VND7*, and their vascular development was aberrant. We conclude that the growth arrest of *WEE1*-deficient plants is due to an extended cell cycle duration in combination with a premature onset of vascular cell differentiation. The latter implies that the plant WEE1 kinase acquired an indirect developmental function that is important for meristem maintenance upon replication stress.

INTRODUCTION

Plant growth depends on meristem activity that provides, through continuous cell division, the cells required for tissue expansion and organogenesis (Harashima and Schnittger, 2010). During development, however, interior and exterior agents attack the meristems, endangering their size, organization, and function. During cell cycle progression, the presence of these agents can lead to faulty cell divisions, causing cells either to lose their meristem identity or to be pushed into programmed cell death (PCD). Massive loss of mitotic cells by aberrant cell divisions results in reduced cell production and decreased growth. Therefore, it is essential that the meristematic cells are preserved by activating cell cycle checkpoints that arrest the cell cycle as long as the stress endures. By contrast, to produce offspring, plants need to sustain growth in a highly competitive environment, even under unfavorable conditions. Hence, they are in need of stress adaptation mechanisms that maintain meristem productivity during stress without compromising meristem function. Discovery and understanding of the molecular basis of these pathways are one of the first steps in the development of stress-resistant crops.

One of the stresses threatening meristem cells is DNA damage. DNA damage can originate from exogenous (such as UV irradiation and heavy metals) or endogenous sources (such as reactive oxygen species and metabolic byproducts) that potentially arrest DNA duplication and cause genomic abnormalities. A progressive accumulation of mutations might initiate uncontrolled growth, provoking cancer in mammals. Although plants are unlikely to develop cancer (Doonan and Sablowski, 2010), they still use the same basic framework to sense and repair damaged DNA. ATAXIA TELANGIECTASIA MUTATED (ATM) and ATM AND RAD3-RELATED (ATR) proteins are the main regulators of the DNA damage pathway and perform functions in plants very similar to those of their orthologs in mammals (Garcia et al., 2003; Culligan et al., 2004, 2006). ATM and ATR both sense DNA damage and induce the coordinated expression of DNA repair and cell cycle–arresting genes. ATM reacts to double-strand breaks (DSBs), whereas ATR primarily responds to single-strand breaks and stalled replication forks.

Many plant DNA repair genes controlled through ATM or ATR have been discovered, but only two genes participating in cell cycle checkpoint activation have been identified, *SOG1* and *WEE1*

[1] Current address: AgroBioInstitute, Buld. Dragan Tzankov 8, 1164 Sofia, Bulgaria.
[2] Current address: Graduate School of Biological Sciences, Nara Institute of Science and Technology, 8916-5 Takayama, Ikoma, Nara 630-0192, Japan.
[3] Address correspondence to lieven.deveylder@psb.vib-ugent.be.
The author responsible for distribution of materials integral to the findings presented in this article in accordance with the policy described in the Instructions for Authors (www.plantcell.org) is: Lieven De Veylder (lieven.deveylder@psb.ugent.be).
[W] Online version contains Web-only data.
www.plantcell.org/cgi/doi/10.1105/tpc.110.082768

(Preuss and Britt, 2003; De Schutter et al., 2007; Yoshiyama et al., 2009). SOG1 is the main transcription factor responsible for the induction of the different ATM/ATR targets upon DNA damage (Yoshiyama et al., 2009). The *WEE1* kinase gene is induced quickly upon DNA stress and interferes directly with cell cycle progression through a mechanism that probably involves inhibitory phosphorylation of the main drivers of the cell cycle, the cyclin-dependent kinases (CDKs) (De Schutter et al., 2007). In yeasts and mammals, WEE1 activity is counteracted by the CDC25 phosphatase, and both are important to time the G2-to-M transition (Gould et al., 1990; Perry and Kornbluth, 2007). Not surprisingly, considering their importance in cell cycle timing, WEE1 and CDC25 are targets of the DNA damage checkpoints that attenuate or halt the cell cycle progression upon genome damage (Harper and Elledge, 2007). Remarkably, in plants, no functional homolog of CDC25 exists, and it has been proposed that its function as cell cycle timer at the G2-to-M transition might have been replaced by plant-specific cell cycle control mechanisms (Boudolf et al., 2006; Dissmeyer et al., 2009, 2010). Nevertheless, despite the absence of a functional CDC25, treatment of *Arabidopsis thaliana* root tips with a replication stress-inducing drug is associated with the phosphorylation of CDKs. This phosphorylation depends on WEE1 because it cannot be observed in *WEE1* knockout (*WEE1*^{KO}) plants (De Schutter et al., 2007). Plants lacking a functional *WEE1* are indistinguishable from wild-type plants when grown under nonstress conditions but are extremely sensitive to replication-inhibiting chemicals, showing a root growth inhibition phenotype (De Schutter et al., 2007). Thus, although WEE1 might lack a function as cell cycle regulator under nonstress conditions, its kinase activity seems to be essential upon replication stress.

Organisms generally suffer from replication stress when substances or conditions interfere with the progression of the replication fork. A typical substance triggering DNA replication stress is hydroxyurea (HU), which targets and inhibits the small subunit of ribonucleotide reductase. Treatment of cells with HU reduces deoxynucleotide triphosphate (dNTP) levels, consequently affecting replication fork progression (Wang and Liu, 2006; Saban and Bujak, 2009). Under these circumstances, it is important that cells monitor replication progression to prevent replication fork stalling with possibly concomitant fork reversal and the occurrence of long stretches of single-stranded DNA (ssDNA) (Lopes et al., 2001, 2003; Postow et al., 2001; Sogo et al., 2002). This mechanism is controlled by the replication checkpoint that handles DNA stress by stabilizing replication forks, inhibiting origin firing, and reducing the replication speed. The latter two events ensure that only reduced levels of dNTPs are needed, thus indirectly averting the occurrence of new stalled replication forks (Alvino et al., 2007; Segurado and Tercero, 2009; Zegerman and Diffley, 2009). In budding yeast and mammals, the replication checkpoint is controlled by MEC1 and RAD53 and the orthologous ATR and CHK1, respectively (Segurado and Tercero, 2009; Zegerman and Diffley, 2009; Branzei and Foiani, 2010). The onset of the S-phase replication checkpoint correlates with an increased phosphorylation of CDKs on Tyr-15 through degradation of the CDC25 phosphatase by the ATR/CHK1 pathway (Zhao et al., 2002; Sørensen et al., 2003; Cook, 2009; Zegerman and Diffley, 2009).

Here, we aimed at understanding why *WEE1*^{KO} plants fail to sustain root growth upon DNA replication stress. In contrast with its anticipated role as a G2/M cell cycle timer, WEE1 is shown to play an essential role during the DNA replication phase in the presence of DNA stress. Absence of WEE1 was found to result in prolonged S-phase duration upon HU treatment, corresponding with the specific accumulation of the kinase in replicating nuclei. In addition, we demonstrate that *WEE1*^{KO} plants suffer from cell death in the vascular meristem because of premature cell differentiation that triggers meristem loss and irregular xylem formation, illustrating that WEE1 safeguards root meristem activity under replication stress.

RESULTS

Cell Cycle, but Not DNA Repair, Is Affected by HU Treatment in *WEE1*^{KO}

Upon treatment with HU, *WEE1*^{KO} *Arabidopsis* plants, with a T-DNA insertion corresponding to a null allele in the *WEE1* gene, show a root growth inhibition phenotype within 24 h, pointing to a role for WEE1 during the DNA replication checkpoint. It had been postulated that the observed growth arrest might result from the inability to arrest mitosis in response to replication defects (De Schutter et al., 2007). To analyze whether WEE1 also plays a role in the G2 DNA damage checkpoint, root growth of *WEE1*^{KO} plants was measured after germination on medium supplemented with 0.6 μg/mL bleomycin (BLM) (Figure 1). As WEE1 is known as a G2/M checkpoint regulator in other organisms (Perry and Kornbluth, 2007), we expected *WEE1*^{KO} plants to be hypersensitive to this DSB-inducing treatment. Surprisingly, *WEE1*^{KO} plants did not display any root growth inhibition. By contrast, *ku70* plants, which lack an important DSB repair protein, showed

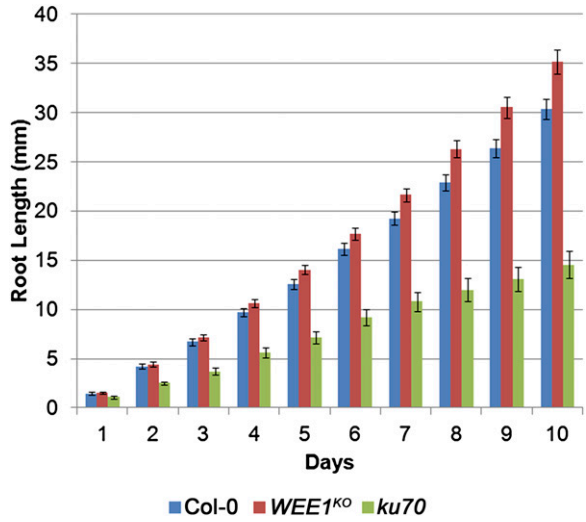

Figure 1. Lack of Hypersensitivity to BLM of *WEE1*^{KO} Plants.

Plants of the indicated genotypes were germinated on 0.6 μg/mL BLM, after which root length was measured at the indicated time points. Data are means ± SE ($n > 21$)

a strong growth phenotype when germinated on BLM, when compared with wild-type seedlings (ecotype Columbia-0 [Col-0]).

Sensitivity of *WEE1*^{KO} plants to HU but not BLM implies that WEE1 is dispensable during the G2 DNA damage response but indispensable during the S-phase checkpoint. To better understand the molecular basis of the root growth inhibitory response phenotype of *WEE1*^{KO} plants upon HU treatment, a microarray experiment was set up to compare the transcriptomes of Col-0 and *WEE1*^{KO} plants grown in the presence or absence of HU. The transcript levels were monitored at two defined time points: 5 and 24 h after treatment with 2 mM HU for the short-term and long-term responses, respectively. These time points were preselected by cDNA-amplified fragment length polymorphism analysis to screen for time points with significant transcriptional changes. As *WEE1* gene transcription is concentrated mainly at the root meristem upon HU treatment (De Schutter et al., 2007), only root tips (<2 to 3 mm) were harvested for RNA extraction.

The samples treated with and without HU were separately analyzed by two-way analysis of variance (ANOVA) for genotype (Col-0 and *WEE1*^{KO}) and time (0, 5, and 24 h). Under control conditions, no genes showed significantly altered expression levels, neither between Col-0 and *WEE1*^{KO}, nor over time, nor for an interaction between time and genotype. The lack of strong transcriptional differences indicates that *WEE1*^{KO} and Col-0 behave similarly in the absence of DNA damage stress, confirming the lack of a root phenotype under control growth conditions. By contrast, 251 genes were differentially regulated upon HU treatment, showing significantly altered gene expression over time. To graphically visualize these transcriptional differences, the significantly altered genes were clustered into seven groups based on their expression levels (see Methods for details) (Figure 2; see Supplemental Data Set 1 online). Gene ontology (GO) overrepresentation analysis of these clusters revealed a significant enrichment for biological processes in four clusters (Figure 2, Table 1). Genes within cluster A displayed a strong (>2.5- to 10-fold change in expression in Col-0 and *WEE1*^{KO} after 24 h) and similar upregulation in both genotypes at both time points after transfer to HU-containing medium (Figure 2A; see Supplemental Data Set 1 online). This cluster was enriched for genes associated with DNA metabolism, DNA repair, and reaction to genotoxic radiation, such as *BRCA1*, *PARP2*, and *XRI1*. Also, *TSO2* and a putative thymidine kinase, both involved in nucleotide metabolism, reacted to the reduction in the dNTP pool caused by HU treatment. All the 18 genes from this cluster had been identified previously as being strongly induced in γ-irradiated seedlings (see Supplemental Table 1 online; Culligan et al., 2006), indicating that upon addition of HU the DNA damage pathway was activated and that a functional copy of *WEE1* was not necessary for sensing DNA stress and transducing the signal to induce DNA repair genes. Similar to cluster A, genes in cluster B were upregulated at both time points upon HU treatment but were less induced (<4-fold induction) (Figure 2B). Like in cluster A, these genes were associated with DNA metabolism and more specifically DNA replication. As HU interferes with both processes, the induced expression of these genes probably resulted from adjustment of the replication process to reduced dNTP levels. Cluster C consisted of genes that were induced transcriptionally only after 24 h in both Col-0 and *WEE1*^{KO} (Figure 2C). The GO

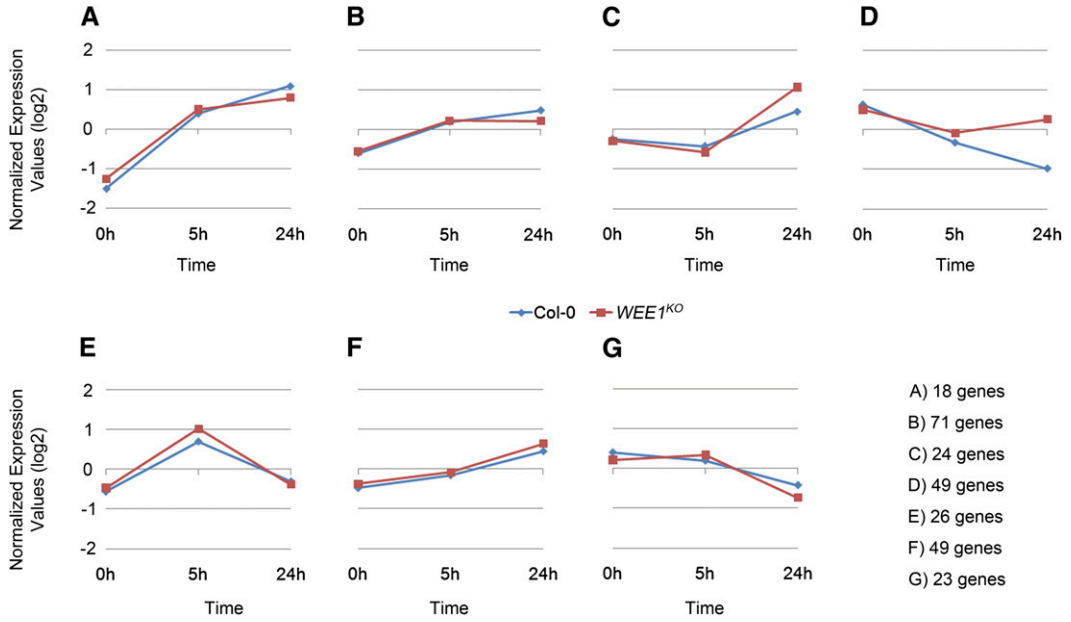

Figure 2. Clustering of Microarray Data of HU-Treated Col-0 and *WEE1*^{KO}.

Genes with significantly altered transcription levels upon HU treatment were clustered into seven different groups based on their expression levels at different time points in mutant and wild-type root tips. Each panel shows the mean normalized expression values of all the genes within the cluster for Col-0 (blue) and *WEE1*^{KO} (red) after 0, 5, and 24 h on HU. The number of genes that each cluster contains is given on the right.

Table 1. GO Analysis of the Different Clusters after Microarray Analysis

Cluster	GO Description	P Value
A	Nucleobase, nucleoside, nucleotide, and nucleic acid metabolic process	4.01E-03
	Nucleic acid metabolic process	1.43E-03
	DNA metabolic process	2.28E-05
	DNA repair	1.84E-06
	DSB repair	1.24E-03
	Cellular response to stimulus	8.15E-04
	Cellular response to stress	3.96E-05
	Response to DNA damage stimulus	1.84E-06
	DNA repair	1.84E-06
	DSB repair	1.24E-03
	Response to ionizing radiation	3.62E-06
	Response to γ-radiation	2.71E-04
	Cell cycle phase[a]	8.16E-03
	M phase[a]	6.09E-03
B	Nucleobase, nucleoside, nucleotide, and nucleic acid metabolic process	4.96E-03
	Nucleic acid metabolic process	1.06E-03
	DNA metabolic process	2.54E-07
	DNA replication	2.05E-04
	DNA methylation on cytosine	3.67E-03
C	Photosynthesis	1.90E-09
	Photosynthesis, light reaction	1.77E-03
	Response to radiation	2.69E-03
	Response to light stimulus	2.69E-03
	Nonphotochemical quenching	1.16E-03
D	Microtubule-based process	2.56E-06
	Microtubule cytoskeleton organization	2.73E-03
	Microtubule based movement	2.93E-03
	Regulation of cell cycle	2.56E-06
E	None	
F	None	
G	None	

After microarray analysis of Col-0 and *WEE1*^{KO} plants treated with HU, the selected genes were divided into seven different clusters that were analyzed for GO enrichment (P value < 0.01). Indentations represent child terms of the above GO terms.

[a]The detection of the M-phase and cell cycle phase GO groups is the result of the presence in this cluster of *XRI1* and *SYN2* that are needed both for DNA repair and M-phase progression.

terms enriched in this gene set were all associated with light stimuli (Table 1), probably linked to the photoinactivating effects of HU on photosystem II in plants (Kawamoto et al., 1994).

Cluster D contained 47 array elements (corresponding to 49 genes) that were downregulated in both genotypes after 5 h on HU. However, cluster D genes reacted differentially at the 24 h time point, showing a further decrease in Col-0, but returning to control levels in the mutant (Figure 2D; see Supplemental Data Set 1 online). Interestingly, within this cluster, 37 out of the 45 array elements that corresponded to a single gene had been previously found to be cell cycle phase-dependently expressed, as supported by GO enrichment analysis (Table 1), with 35 of them peaking during the M phase (see Supplemental Table 2 online; Menges et al., 2003). As described previously, downregulation of M-phase genes in the root meristem of control plants results from cell cycle synchrony imposed by the HU treatment (Cools et al., 2010). Synchrony is achieved through HU-induced depletion of the dNTP pool, resulting in a transient accumulation of cells at the G1-to-S transition. An increase in intracellular dNTPs through salvage pathways probably increases the level of nucleotides above a threshold level, after which cells synchronously resume cell division. In this synchronization system, Col-0 root tip cells progress into mitosis 16 h after HU treatment, and enter S phase around 6 and 22 h. At these two time points, cells are depleted for G2/M cells, explaining the reduction in M-phase gene expression at the 5- and 24-h time points in the microarray experiment (Cools et al., 2010). Although the statistical analysis of the microarray data did not allow us to call the altered kinetics of G2/M gene transcription in *WEE1*^{KO} after HU treatment significantly different from that seen in Col-0, the data suggested an altered cell cycle regulation at the 24-h time point in *WEE1*^{KO} plants in the presence of HU.

WEE1^{KO} Plants Display Altered S-Phase Kinetics

The HU-imposed cell cycle synchronization allowed us to investigate in more detail the possibility of altered cell cycle regulation in *WEE1*^{KO} plants upon replication stress. Root tips were collected for transcript analysis at 2-h time intervals from 0 to 22 h after transfer to HU. RNA levels were measured with the nCounter analysis system (NanoString Technologies) that allows a direct multiplexed analysis of selected transcripts (Geiss et al.,

2008). When compared with Col-0, *WEE1^{KO}* plants initially displayed identical cell cycle progression, as exemplified by the transcription profile of the S-phase marker gene *CYCA3;1* (Figure 3A), showing that *WEE1^{KO}* is susceptible to HU synchronization. As indicated by the expression profiles of *CYCA3;1* and *histone H4*, DNA replication initiated around 4 to 6 h after transfer to HU (Figures 3A and 3B). Also, the mid-S-phase marker gene *histone H2B* was induced at the same time in Col-0 and *WEE1^{KO}* (Figure 3C). However, altered S-phase kinetics became apparent when the transcription of the late-S-phase marker gene *histone H1* was examined. Like *histone H4* and *H2B*, *histone H1* was induced simultaneously in both backgrounds but had a prolonged window of expression and superinduction (10 to 22 h) in *WEE1^{KO}* (Figure 3D). Together, the histone gene expression kinetics imply that *WEE1*-deficient plants progress normally into S phase but encounter stress during the replication process. Accordingly, downstream cell cycle events are clearly affected in the *WEE1^{KO}* plants, as illustrated by the attenuated and delayed expression profiles of the G2/M marker genes *CYCA2;1* (peaks at 18 h versus 14 h in Col-0) and *CYCB1;2* (peaks at 20 h versus 16 h in Col-0) (Figures 3E and 3F). Genes present in the cluster D of the microarray analysis (*CYCA1;1*, *CYCB2;1*, and *CYCB2;4*) showed similar delayed expression kinetics (see Supplemental Figure 1 online), confirming the earlier observations of the microarray analysis and pointing toward a delayed progression through mitosis in *WEE1^{KO}* plants. Despite the prolonged S phase, the peaks of early G2 (*CYCA2;1*) and late G2/M (*CYCB1;2*) genes were separated by 2 h in both Col-0 and mutant, indicating that mainly the S-phase progression is sensitive to the HU treatment in *WEE1^{KO}*.

Among all G2/M genes tested, *CYCB1;1* displayed a unique transcriptional profile (Figure 3G). Previously, *CYCB1;1* expression had been connected with a role in the DNA damage response because its expression was found to be strongly induced and stabilized during γ-irradiation (Culligan et al., 2006). In contrast with the related *CYCB1;2*, *CYCB1;1* levels were not downregulated during S phase in HU-synchronized Col-0 root tips (Cools et al., 2010). However, in *WEE1^{KO}*, *CYCB1;1* was rather strongly transcriptionally activated at the start of replication (Figure 3G), as observed for DNA damage genes, such as *BRCA1* (Figure 3H), and had lost the typical induction kinetics of G2/M genes.

WEE1 Controls S-Phase Progression during Replication Stress

In contrast with its anticipated role as timer of the G2-to-M transition upon the occurrence of DNA stress (Perry and Kornbluth, 2007; Geiss et al., 2008), our data indicated that *Arabidopsis WEE1* rather plays an important part during DNA replication. Correspondingly, within the root synchronization system, *WEE1* transcripts accumulated after 4 to 6 h, the time of S-phase onset, with kinetics comparable to those of the S-phase marker *CYCA3;1* (Figure 4A). Furthermore, similar to DNA repair genes, *WEE1* levels remained induced during the whole period of the HU treatment.

To confirm that *WEE1* specifically accumulates during S phase upon replication stress, *WEE1^{KO}* plants were transformed with a *P$_{WEE1}$:GFP-WEE1* complementation construct. Transgenic plants harboring the construct partially rescued the HU hypersensitivity of the *WEE1*-deficient plants (Figures 4B and 4C). In the absence of DNA stress, only background fluorescence was detected in the root. By contrast, a nuclear-localized GFP-WEE1 signal could be observed in the vascular meristem cells after 24 h treatment with HU, corresponding with its previously reported expression pattern (Figure 4C; De Schutter et al., 2007). To pinpoint the cell cycle phase at which the GFP-WEE1–positive cells accumulate, fluorescent cells were separated from negative ones by fluorescence-activated cell sorting, either from control root tips (not treated with HU) or root tips of plants treated with HU for 48 h. Subsequently, nuclei were extracted from the sorted cells, and their DNA content was measured by flow cytometry. In the total population of nuclei within the root tip of untreated plants, two distinct populations were observed with a 2C and 4C DNA content, corresponding to G1 and G2 nuclei, respectively (Figure 4D). Because of the lack of a GFP signal in the absence of DNA stress, no GFP-positive nuclei could be detected. When transferred to HU, the relative abundance of nuclei with a DNA content in between 2C and 4C, corresponding to S-phase nuclei, increased (Figure 4E). When the DNA content of GFP-WEE1–positive cells was measured, a single population of nuclei was observed, localized precisely between the 2C and 4C peaks (Figure 4E). These data substantiate the hypothesis that WEE1 operates specifically in replicating cells that undergo replication defects.

HU Triggers Vascular Cell Death in *WEE1^{KO}* Root Meristems

Treatment of plants with DSB-inducing drugs commonly results in death of the root stem cells (Fulcher and Sablowski, 2009; Furukawa et al., 2010). As *WEE1^{KO}* plants show strong growth retardation in the presence of HU, they were tested for the occurrence of dead cells. Plants were transferred to HU-containing medium and stained at different time points with propidium iodide (PI) that stains the walls of living cells but penetrates dead cells. As HU can be used to invoke root synchronization, the appearance of cell death could be correlated with cell cycle progression. At the first time points analyzed (3 to 8 h), no PI-stained cells were detected in both Col-0 and *WEE1^{KO}* root meristems (Figure 5A). By contrast, at the moment that cells started accumulating in mid-S-phase (9 to 10 h), the first dead cells were visible in the mutant, in contrast with Col-0, where no PI-positive cells were observed (Figure 5A). The timing of cell death appearance suggested that defective S-phase progression might lie at the basis of the phenotype.

To investigate the spatial occurrence of cell death, plants were transferred for 24 h to medium supplemented with HU and again stained with PI. A large amount of dead cells was seen throughout the *WEE1^{KO}* meristem but not in Col-0. Interestingly, this spatial cell death pattern differed clearly from that provoked by DSBs, such as after treatment with BLM (Figure 5B), which induced cell death specifically in the stem and progenitor (StPr) zone (Fulcher and Sablowski, 2009; Furukawa et al., 2010). By contrast, dead cells in the meristem of *WEE1^{KO}* plants did not occur in the stem cells but were located in the transiently amplifying (TA) region of the vascular tissue (Figure 5A). To

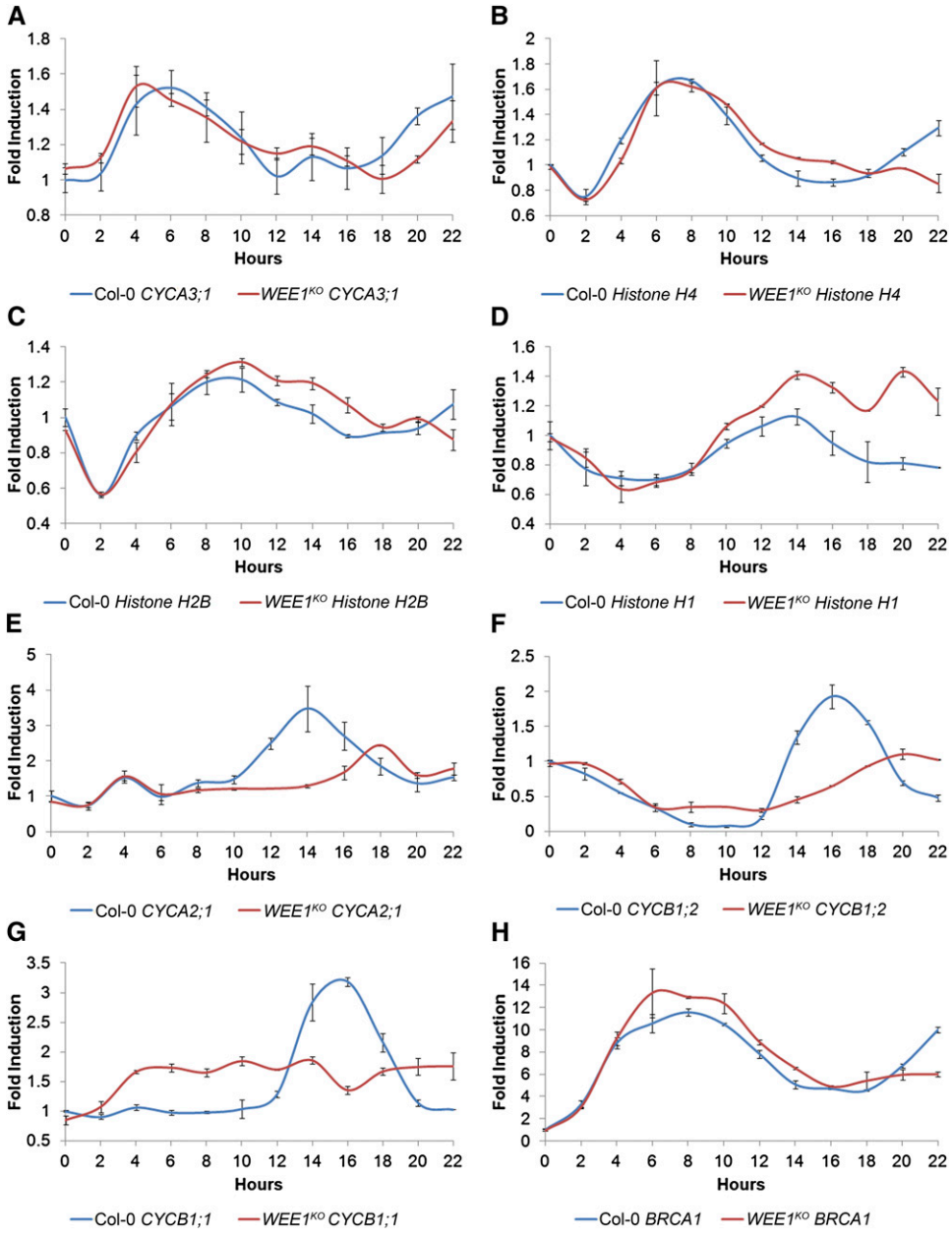

Figure 3. Time-Course Analysis of Cell Cycle Genes in HU-Synchronized Col-0 and *WEE1*^{KO} Root Tips.

Transcript levels were measured by nCounter analysis. Fold induction levels of the different transcripts are presented for Col-0 (blue) and *WEE1*^{KO} (red). *EMB2386*, *PAC1*, and *RPS26C* were used as reference genes. Transcript levels were rescaled to the level in Col-0 at 0 h (=1). Time after treatment with HU is given on the horizontal axis. Data are means ± SE.

(A) *CYCA3;1*.
(B) *Histone H4*.
(C) *Histone H2B*.
(D) *Histone H1*.
(E) *CYCA2;1*.
(F) *CYCB1;2*.
(G) *CYCB1;1*.
(H) *BRCA1*.

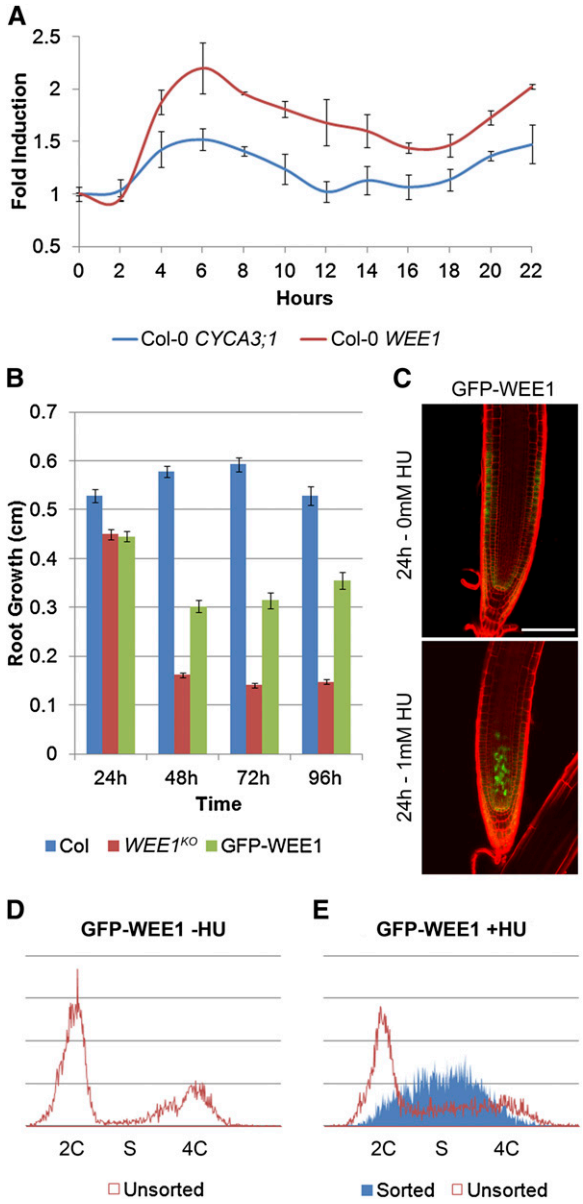

Figure 4. Stabilization of WEE1 during S Phase upon Replication Stress.

(A) Transcript analysis of *CYCA3;1* (blue) and *WEE1* (red) in HU-synchronized Col-0 root tips. Data are means ± SE.

(B) Daily growth of Col-0 (blue), *WEE1*^{KO} (red), and P_{WEE1}:GFP-WEE1 (green) roots after transfer to 1 mM HU. Growth was followed until 4 d after transfer. Data are means ± SE ($n > 37$).

(C) Confocal microscopy of the P_{WEE1}:GFP-WEE1 line transferred for 24 h to 0 mM HU (top) and 1 mM HU (bottom). Epidermis-localized green signal at 0 mM HU is due to background signal. Nuclear GFP-WEE1 signal in the vascular cells was seen after treatment with 1 mM HU. Bar = 0.1 mm.

(D) Flow cytometry profile of unsorted and untreated P_{WEE1}:GFP-WEE1 root tips. 2C, 4C, and S indicate G1, G2, or S-phase nuclei, respectively.

(E) Flow cytometry profile of unsorted (red) and sorted GFP-WEE1 (blue) root tips treated for 24 h with 10 mM HU.

investigate whether this specific cell death localization was caused only by replication stress or also depended on *WEE1* deficiency, we increased the HU concentrations to a level that induces cell death in Col-0 plants (5 mM HU). If cell death localization depended solely on HU, the cell death pattern in Col-0 would be expected to be the same as that of the *WEE1*^{KO} plants. Surprisingly, the observed pattern resembled that of plants suffering from DSBs, with cell death restricted to the StPr cells (Figure 5C). Also, *WEE1*^{KO} plants now displayed dead cells around the quiescent center, in addition to those in the vascular TA region. Remarkably, cell death in the StPr zone was not limited to vascular tissue. These data indicate that increased levels of HU indirectly cause cell death in Col-0, probably by the secondary occurrence of DSBs with dead StPr cells as a consequence. Moreover, together with the lack of a root growth phenotype in *WEE1*^{KO} plants growing on BLM (Figure 1), it implies that WEE1-independent pathways cope with DSBs in the StPr cells and that WEE1 preferentially protects the vascular TA zone upon replication stress.

Previously, WEE1 had been shown to operate downstream of ATM and ATR (De Schutter et al., 2007). Both ATM and ATR have been demonstrated to be required for the onset of cell death in the StPr cells upon DNA damage (Fulcher and Sablowski, 2009; Furukawa et al., 2010). To investigate the occurrence and pattern of cell death upon replication stress in *atm-1* and *atr-2* mutant plants, they were treated for 24 h with 1 mM HU. As *atm-1* plants are not hypersensitive to replication stress, they evidently did not suffer from cell death in the root meristem (Figure 5D). By contrast, *atr-2* plants, which are highly sensitive to HU (Culligan et al., 2004), exhibited severe cell death (Figure 5D). The cell death phenotype in *atr-2* plants was more severe than that in *WEE1*^{KO} plants and also occurred in the stem cell zone. This observation can be attributed to the fact that besides its inability to induce *WEE1* expression, *atr-2* also fails to induce the DNA repair machinery to repair the afflicted DNA. Nevertheless, the common cell death phenotype in the vascular TA zone in *WEE1*^{KO} and *atr-2* plants indicates that the ability of WEE1 to inhibit cell death in the distal vascular meristem upon replication stress depends on ATR.

WEE1 Is Required to Prevent Premature Tracheary Element Differentiation upon Replication Stress

Because stem cells are the first to react to DNA damage, the lack of dead stem cells in *WEE1*^{KO} plants indicated that the root growth arrest might be unrelated to the occurrence of severe DNA damage. Indeed, upon HU treatment, no substantial differences were observed between Col-0 and *WEE1*-deficient plants when examining DNA damage hallmarks, such as the occurrence of DNA fragmentation or increased recombination (see Supplemental Figure 2 online). Because dead cells were specifically observed in the provascular zone and PCD is an intrinsic process of vascular maturation, the cell death in *WEE1*^{KO} plants could reflect the onset of premature differentiation in the vascular tissue, rather than DNA damage–induced PCD, as suggested previously (Ricaud et al., 2007; Fulcher and Sablowski, 2009). Therefore, we took a closer look at genes that function in tracheary element (TE) differentiation (Turner et al., 2007).

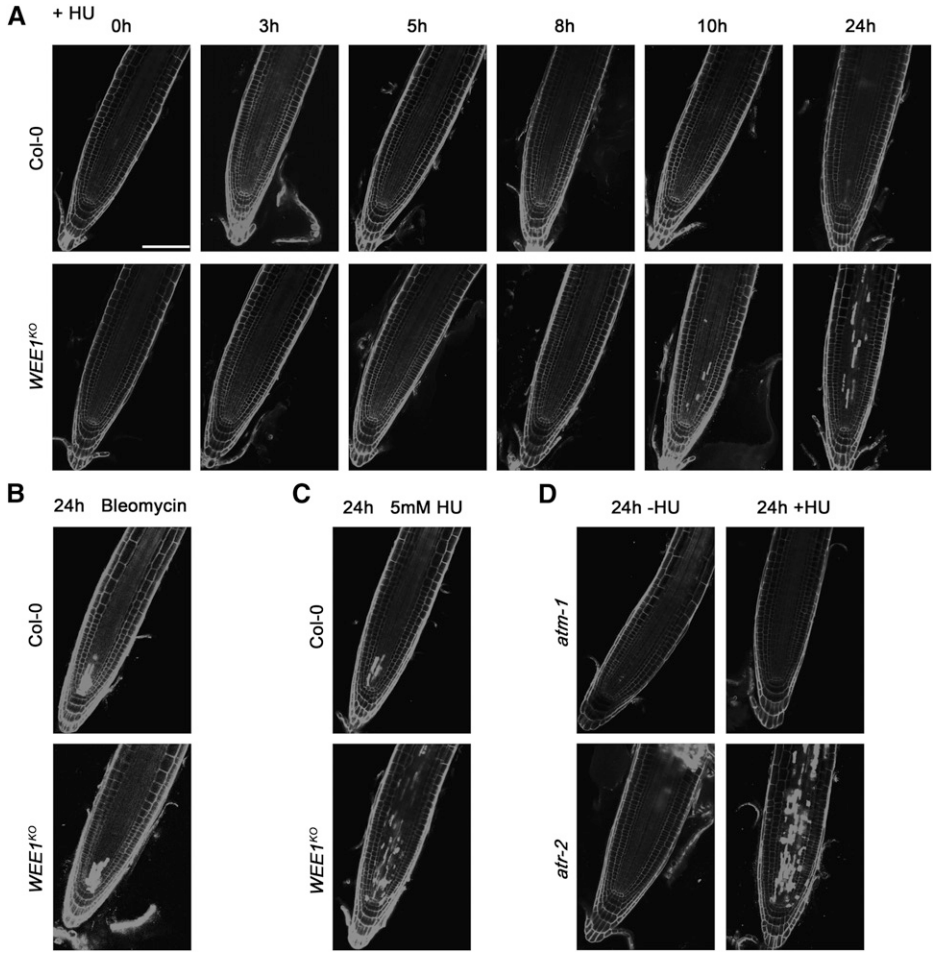

Figure 5. Vascular Cell Death Phenotype of *WEE1*^{KO} roots upon Replication Stress.

(A) Time course of Col-0 and *WEE1*^{KO} root tips transferred to HU and stained with confocal microscopy. Dead cells are stained with PI. Time after transfer to HU medium is indicated above the root tips.
(B) PI staining of Col-0 and *WEE1*^{KO} after treatment with 0.6 μg/mL BLM for 24 h.
(C) PI staining of Col-0 and *WEE1*^{KO} grown for 24 h on 5 mM HU.
(D) PI staining of *atm-1* and *atr-2* transferred either for 24 h to control medium or 1 mM HU.

Transcripts of five of these genes (*CESA4*, *IRX1*, *IRX3*, *XCP1*, and *XCP2*) were quantitatively measured by real-time PCR in both Col-0 and *WEE1*^{KO} 0, 24, and 48 h after treatment with HU. Whereas transcript levels of the TE differentiation genes decreased slightly upon HU treatment in Col-0, they increased in *WEE1*^{KO} (Figure 6A; see Supplemental Figure 3 online). The latter suggested that *WEE1*^{KO} plants undergo premature TE differentiation upon HU treatment. To further test this hypothesis, a *VND7* reporter construct (*VND7pro:GUS*) was introgressed into a *WEE1*^{KO} background. VND7 is a transcription factor implicated in xylem differentiation (Kubo et al., 2005; Yamaguchi et al., 2008, 2010). Under normal growth conditions, the root meristem shows no *VND7* expression in Col-0 and *WEE1*^{KO} plants (Kubo et al., 2005) (Figure 6B). After treatment of *VND7pro:GUS* lines with 1 mM HU for 24 h, β-glucuronidase (GUS) staining could be observed specifically within the root meristem of the *WEE1*^{KO} plants (Figure 6B). At higher HU concentration (2.5 mM HU), Col-0 root tips occasionally showed an individual cell with weak *VND7* expression. However, expression was much more pronounced in *WEE1*^{KO}, showing many cells with a strong *VND7* induction, demonstrating the molecular onset of vascular differentiation.

Protoxylem formation is inhibited by cytokinin treatment (Mähönen et al., 2006). If premature protoxylem differentiation were at the basis of the observed cell death after HU treatment in *WEE1*^{KO}, N_6-benzyladenine (BA) treatment would reduce the vascular cell death phenotype upon replication stress. To test this hypothesis, *WEE1*^{KO} plants were transferred to medium containing no drugs, 1 mM HU, 100 nM BA, or a combination of HU and BA. After 24 h, a reduction in the number of PI-stained cells was visible in plants treated with HU in combination with BA, compared with plants treated with 1 mM HU only (Figure 7; see Supplemental Figure 4 online). This effect was even more obvious at the 48-h time point, when almost no dead cells were visible

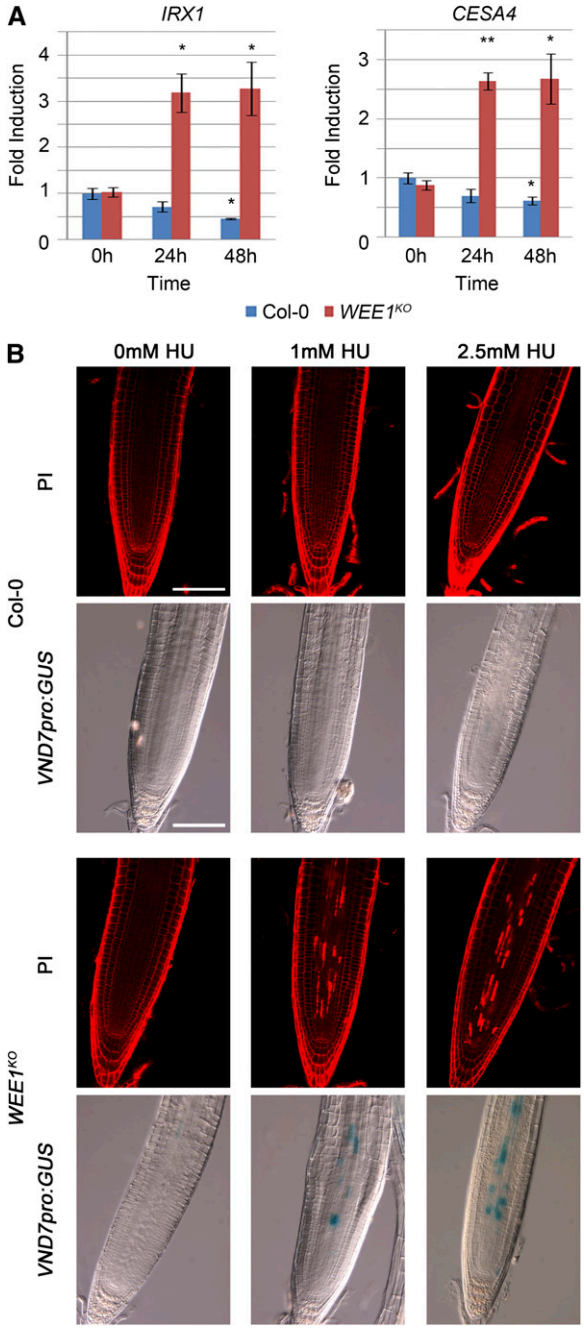

Figure 6. Premature Vascular Differentiation Induced by Replication Stress in *WEE1*^{KO} Plants.

(A) Tracheary element differentiation genes are induced in *WEE1*^{KO} root tips upon replication stress. qRT-PCR transcript analysis of *IRX1* and *CESA4* in Col-0 and *WEE1*^{KO} 0, 24, and 48 h after HU treatment. *EMB2386*, *PAC1*, and *RPS26C* were used as reference genes. The transcript levels were rescaled to the level in Col-0 at 0 h (=1). Asterisks indicate significantly altered transcription levels compared with the 0-h time point (*P value < 0.05; **P value <0.001). Data are means ± SE (n = 4).

(B) Confocal microscopy of Col-0 and *WEE1*^{KO} plants after PI staining to detect cell death. Col-0 and *WEE1*^{KO} harboring a *VND7pro:GUS* construct were stained with GUS. Plants were treated either with 0 mM (left), 1 mM HU (center), or 2.5 mM HU (right) for 24 h. Bars = 0.1 mm.

after BA and HU treatment. To connect the ectopic expression of *VND7*, and consequent vascular differentiation, with the observed cell death in *WEE1*^{KO}, we analyzed whether the addition of BA attenuated the *VND7* induction in *WEE1*^{KO} after HU treatment. Indeed, 24 h after transfer to HU medium supplemented with BA, *VND7* expression was strongly reduced in the *WEE1*^{KO} root tip (Figure 8A). Together, these data strongly indicate that replication stress-induced cell death and xylem differentiation, due to the lack of *WEE1*, are coupled events.

Absence of WEE1 Results in Aberrant Vascular Differentiation upon Long-Term Replication Stress

Because of the observed link between replication stress and TE differentiation, the vascular tissue was examined in *WEE1*^{KO} plants after a prolonged and strong HU treatment. Wild-type plants displayed normally organized protoxylem and metaxylem development after 4 d of growth on HU. By contrast, in *WEE1*^{KO} plants, the xylem was disorganized with interrupted and additional xylem rows (Figures 8B and 8C). The presence of multiple and extra xylem rows immediately above the root meristem indicates that vascular meristem cells in *WEE1*^{KO} plants trigger their maturation program prematurely. These data clearly demonstrate a function for WEE1 as inhibitor of premature vascular differentiation under replication stress conditions.

DISCUSSION

WEE1 Controls S-Phase Progression under Replication Stress

DNA damage checkpoint research is far more advanced in nonplant organisms, illustrated by the large number of known regulators contributing to the cell cycle arrest and DNA repair mechanisms activated upon DSBs or replication defects in yeasts and mammals. Although the presence of a functional ATM and ATR suggests that the main mechanisms controlling the DNA damage response in plants might be similar, homologs of several key signaling components have not been identified in the *Arabidopsis* genome (Cools and De Veylder, 2009). The mechanisms by which yeast and mammalian cells arrest their proliferation in response to DNA stress depend on the cell cycle phase at which the cell resides at the moment the damage is inflicted. Independently of the followed pathway, the common goal is inhibition of the CDK activity to prevent cell cycle progression in the presence of damaged or incompletely replicated DNA. When damage occurs during replication, the intra-S checkpoint is activated, correlating with the accumulation of P-loop–phosphorylated inactive CDKs, probably through inhibition of CDC25 (Zegerman and Diffley, 2009). The CHK1-CDC25 pathway dominates S-phase regulation in mammals and budding yeast during replication stress, but no direct role has been demonstrated for its counterpart WEE1. By contrast, we

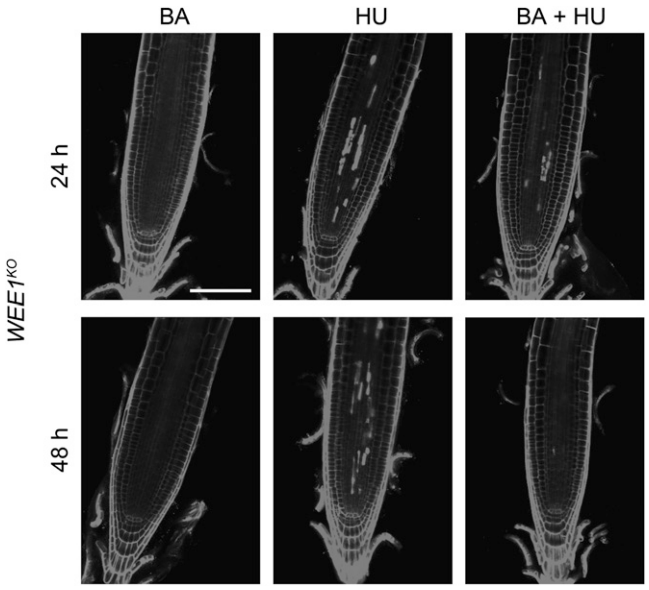

Figure 7. Reduced Vascular Cell Death in *WEE1*^{KO} by BA.

PI staining to detect cell death in *WEE1*^{KO} plants treated for 24 h (top) or 48 h (bottom) with 100 nM BA (left), 1 mM HU (center), or 1 mM HU and 100 nM BA (right). To show the reproducibility of the experiment, several treated root tips are shown in Supplemental Figure 4 online. Bar = 0.1 mm.

identified *WEE1* as an essential intra-S-phase checkpoint gene in *Arabidopsis*, as demonstrated by the delayed progression through S phase in synchronized *WEE1*^{KO} root tips and the specific accumulation of its gene product in replicating nuclei upon HU treatment. As there is no functional CDC25 or CHK1 homolog in *Arabidopsis*, the upregulation of *WEE1* during S phase and the hypersensitivity of the *WEE1*^{KO} mutant to replication stress put WEE1 forward as the main regulator of the S-phase checkpoint in plants.

Plants without a functional *WEE1* gene show a superinduction and prolonged transcription of different histone genes after treatment with HU. This result implies a problematic S-phase progression with a delayed entry into G2 as a consequence. By contrast, the timing between G2 and G2/M progression (2 h) was not extended in *WEE1*^{KO} compared with Col-0 plants. Upon treatment with HU, cells need to adjust replication with the depleted dNTP pools. Generally, dNTP depletion is counteracted by slowing down replication and delaying the initiation of replication origins (Willis and Rhind, 2009), which is accomplished by reducing the CDK activity during S phase through the ATR-CHK1 pathway that inactivates CDC25 (Cook, 2009; Willis and Rhind, 2009; Zegerman and Diffley, 2009). Because of the absence of functional *CDC25* and *CHK1* genes in plants, we hypothesize a role for WEE1 during DNA stress as coordinator of CDK activity with replication fork progression and/or origin firing. Disruption of the CDK activity–controlling pathway in budding yeast during HU treatment by means of a mutated *Rad53* (the ortholog of *CHK1*) causes the checkpoint mutants to produce long stretches of ssDNA and fork reversal, forming structures similar to Holliday junctions (Lopes et al., 2001; Sogo et al., 2002; Branzei and Foiani, 2010). Similarly, the observed replication difficulties in *WEE1*^{KO} plants might arise from the inability to attenuate sufficiently DNA replication to the limited dNTP levels. The lack of checkpoint activity and CDK control probably prevents inhibition of origin firing and/or deceleration of replication. This will eventually increase the number of stalled replication forks in *WEE1*^{KO}, with potentially concomitantly extended ssDNA regions or fork reversal as a result. Evidently, the aggravation of replication problems takes more time to repair, with a cell cycle delay as a consequence.

Whereas the WEE1 protein is an essential checkpoint regulator under replication stress, its presence appears to be dispensable for the response to other types of DNA damage, such as DSBs. If WEE1 is still an element of the DSB checkpoint, its role will be, at most, redundant with other mechanisms. Currently, these mechanisms are still unknown, but likely candidates might be found among the class of cell cycle inhibitors (CKIs). Plants have two classes of CKIs (KIP-RELATED PROTEINS and SIAMESE/SIAMESE-RELATED) with a limited sequence similarity to the mammalian Cip/Kip CDK inhibitors (De Veylder et al., 2001; Churchman et al., 2006) of which some members are strongly

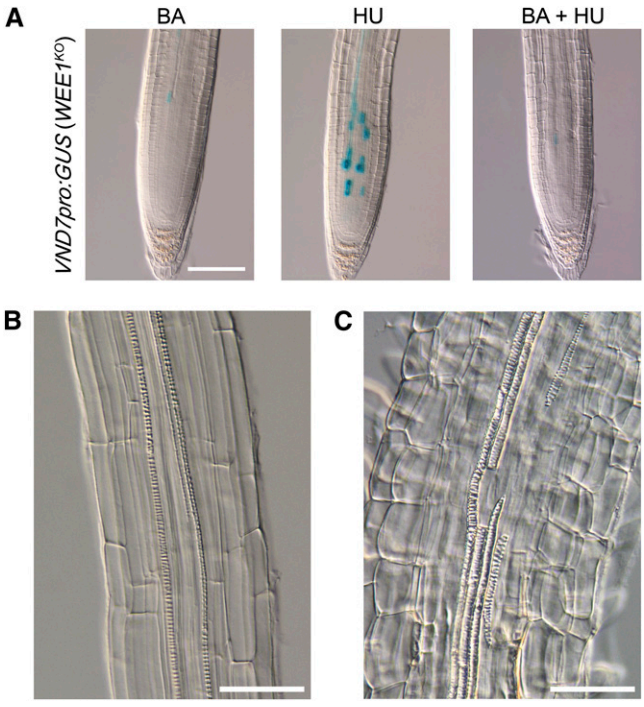

Figure 8. Aberrant Vascular Differentiation in *WEE1*^{KO} Plants Caused by HU Treatment.

(A) GUS staining of *VND7pro:GUS* (*WEE1*^{KO}) after 24 h treatment with 100 nM BA (left), 2.5 mM HU (center), or a combination of both BA and HU (right). Bar = 0.1 mm.

(B) Microscopy analysis of vascular development of Col-0 treated for 4 d with 2.5 mM HU. Bar = 0.05 mm.

(C) Microscopy analysis of aberrant vascular development of *WEE1*^{KO} plants treated for 4 d with 2.5 mM HU. Bar = 0.05 mm.

transcriptionally induced by genotoxic stress treatments (Peres et al., 2007).

WEE1 and Vascular Differentiation

Besides halting S-phase progression, the absence of a functional WEE1 protein in the presence of replication stress causes clear developmental defects. Upon addition of HU, dead cells accumulate in the root tip of *WEE1^{KO}* plants. These cells are located predominantly in the vascular meristem, in contrast with DSB-inducing treatments that mainly target the stem cells of all root cell types (Fulcher and Sablowski, 2009; Furukawa et al., 2010). PCD is an intrinsic part of vascular development (Turner et al., 2007); indeed, through *VND7* promoter activity measurements, cell death in the *WEE1^{KO}* plants was associated with the onset of the vascular differentiation program. Moreover, cell death could be reduced by cytokinin treatment that is known to inhibit protoxylem differentiation in *Arabidopsis* roots (Mähönen et al., 2006). PI-stained *WEE1^{KO}* cells could be observed within 10 h after HU treatment and were positioned close to the stem cells, indicating that their position in the meristem arose by a premature onset of vascular differentiation, rather than because of shrinkage of the meristem as a result of the described effect on cell cycle duration. Likewise, ectopic expression in the meristem of *VND7* and other vascular differentiation genes, normally only observed in the immature xylem cells outside the meristem (Kubo et al., 2005; Yamaguchi et al., 2008, 2010), hints at a premature onset of vascular differentiation and likely explains the irregular xylem organization in *WEE1^{KO}* roots upon long-term HU treatment. Interestingly, in contrast with the *WEE1^{KO}* plants, the Col-0 roots showed a decrease in expression of vascular differentiation genes within the root meristem upon replication stress, which might be correlated with the transcriptional induction of *WEE1* in the vascular meristem (De Schutter et al., 2007). This observation is corroborated on the protein level by the WEE1 stabilization after HU treatment in the vascular meristem cells. Altogether, these data indicate an indirect developmental role for WEE1 upon replication stress as an inhibitor of premature xylem formation. Strikingly, even high HU concentrations could not elicit the vascular cell death response in control plants. Rather, cell death was limited to the root initial cells, very similarly to that observed upon exposure to DSB-inducing drugs (Curtis and Hays, 2007; Fulcher and Sablowski, 2009; Furukawa et al., 2010). Hence, WEE1 is a very potent safeguard of the mitotic status of vascular cells, specifically toward replication stress.

The specific prevascular cell death upon HU application suggests that replication stress might be an intrinsic part of the vascular differentiation process. In agreement, the treatment of cells of zinnia (*Zinnia elegans*) with aphidicolin, a compound that induces replication stress through the inhibition of DNA polymerases, promoted their differentiation into tracheary elements (Mourelatou et al., 2004). In addition, the gene *EFFECTOR OF TRANSCRIPTION2*, implicated in xylem differentiation, has an endonuclease domain responsible for making single-strand cuts within the DNA and is essential for the protein's role in vascular development (Ivanov et al., 2008), suggesting that the occurrence of ssDNA might start xylem differentiation. Thus, WEE1 and replication stress apparently play an antagonistic role in the development of vascular tissue, in which WEE1 prevents loss of vascular meristem identity upon replication stress to sustain meristem activity.

Plant WEE1 and CDC25 during Evolution

In contrast with other organisms, in *Arabidopsis*, WEE1 and other DNA damage checkpoint proteins are not essential during unperturbed cell cycle conditions (Cools and De Veylder, 2009), as exemplified by the lack of any phenotype of *WEE1^{KO}* plants under nonstress growth conditions (De Schutter et al., 2007). Nevertheless, the amino acid residues of CDKs targeted for phosphorylation by WEE1 seem to be conserved, and their substitution into phosphorylation-mimicking sites results in a severe growth phenotype due to a cell cycle arrest (Dissmeyer et al., 2009), implying that the inhibitory function of the P-loop is conserved. However, whereas in other model species control of CDK activity through P-loop phosphorylation/dephosphorylation is used for timing of the G2-to-M transition (Gould et al., 1990; Perry and Kornbluth, 2007), plants use apparently other mechanisms to time their M phase onset, likely with the plant-specific B-type CDKs, because their activity is required for progression through the G2-to-M transition (Porceddu et al., 2001; Boudolf et al., 2004; Cools et al., 2010). Considering the number of striking parallels between the plant B1-type CDKs and mammalian CDC25, it has been suggested previously that during evolution, CDC25 control of the onset of mitosis might have been replaced in the plant kingdom by B1-type CDKs (Boudolf et al., 2006). Our work strengthens the case for a lack of G2-to-M control through P-loop phosphorylation because *WEE1* transcript abundance peaks during S-phase progression, whereas its associated kinase activity is only required in times of replication stress. Moreover, its importance in maintaining meristem structure through the inhibition of premature vascular cell differentiation suggests an indirect role for WEE1 as a developmental regulator. It indicates that during evolution, WEE1 and CDC25 have lost their function as antagonistic checkpoint controllers in plants, combined with the acquisition of a developmental role for WEE1. Once such a developmental role had been established, there might have been no reason to retain a functional *CDC25* in the genome. Consequently, WEE1 controls two important processes influencing the meristem integrity under HU conditions: it controls meristem size by affecting cell cycle duration, and it ensures meristem structure by preventing premature differentiation. Hence, we conclude that WEE1 is an essential element to ensure meristem maintenance during replication stress.

METHODS

Plant Materials and Growth Conditions

Arabidopsis thaliana plants (ecotype Col-0) were grown in vitro vertically under long-day conditions (16 h light/8 h darkness) at 21°C on half-strength Murashige and Skoog (2.151 g/L) (Duchefa), 10 g/L sucrose, and 0.5 g/L MES, pH 5.7, adjusted with 1 M KOH and 10 g/L agar. For HU treatments, plants were grown for 7 d (2 d of germination and 5 d of growth) on control medium and then transferred either to fresh control medium or HU-containing media (Sigma-Aldrich). The HU concentration used was 1 mM unless stated otherwise and that of BLM (Duchefa) was

0.6 μg/mL, whereas BA (Duchefa) was brought to a final concentration of 100 nM. Whenever synchronization conditions (Cools et al., 2010) were used, plants were grown vertically under continuous light conditions at 21°C with 1× Murashige and Skoog medium (4.302 g/L), 10 g/L sucrose, 0.1 g/L myo-inositol, 0.5 g/L MES, 100 μL thiamine hydrochloride (10 mg/mL), 100 μL pyridoxine (5 mg/mL), and 100 μL nicotinic acid (5 mg/mL), pH 5.7, adjusted with 1 M KOH and 10 g/L agar. Seeds were placed on a nylon mesh (20 μm pore size) (Prosep) and transferred after 1 week to plates with 2 mM HU. The root growth response of Col-0 and *WEE1*^{KO} plants grown in the presence of 2 mM HU on nylon was identical to that of plants growth directly on medium supplemented with 1 mM HU (data not shown).

The P$_{WEE1}$:GFP-WEE1 construct was created with Gateway technology (Invitrogen). An N-terminal fusion of GFP with the WEE1 protein under the control of the endogenous *WEE1* promoter (−605 to −1) was constructed with the MultiSite Gateway three-fragment vector construction kit (Invitrogen). Three different vectors were used (*WEE1* promoter in pDONRP4P1R [Invitrogen], GFP in pDONR221 [Invitrogen], and WEE1_ORF in pDONRP2RP3 [Invitrogen]) and were cloned in the pK7m34GW destination vector (Karimi et al., 2005) by a MultiSite LR reaction. After transformation of the sequenced constructs to *Agrobacterium tumefaciens*, *WEE1*^{KO} plants were transformed by floral dip (Clough and Bent, 1998). Kanamycin-resistant plants were selected and analyzed for their ability to complement the *WEE1*^{KO} phenotype on HU.

GU-US (*uidA* recombination), *ku70*, *atm-1*, *atr-2*, *VND7pro:GUS*, and *WEE1*^{KO} (*wee1-1* and *wee1-2*) lines had been described previously (Swoboda et al., 1994; Riha et al., 2002; Garcia et al., 2003; Culligan et al., 2004; Kubo et al., 2005; De Schutter et al., 2007). *wee1-1* and *wee1-2* plants were pooled in the microarray experiment. Nanostring and phenotypic analysis were done with *wee1-1*.

Microarray Analysis

Plant lines and growth conditions were as described above. Col-0 and *WEE1*^{KO} (*wee1-1* and *wee1-2*) seeds were germinated on control medium on a nylon mesh and transferred 5 d after germination to control medium or medium supplemented with 2 mM HU. All sampling points were collected over four independent biological repeats for Col-0, two independent repeats for *wee1-1*, and two for *wee1-2*. For each independent time point of each experiment ±50 root tips (<2 to 3 mm) were collected and frozen in liquid nitrogen. RNA was extracted from root tissue with TriZol reagent (Invitrogen) and purified with the RNeasy plant mini kit (Qiagen). The RNA of two independent experiments for Col-0 and *WEE1*^{KO} were subsequently pooled and used for microarray analysis. A total of 24 samples were individually hybridized to microarrays, representing two genotypes (Col-0 and *WEE1*^{KO}) grown under two conditions (−HU and +HU), harvested at three time points (0, 5, and 24 h), in duplicate. Out of 5 μg of total RNA, biotinylated-copy RNA was produced, fragmented, and hybridized to ATH1 arrays (Affymetrix). Washing, detection, and scanning were done as described previously (Hennig et al., 2003). Array data were made available as Affymetrix.CEL files, and the quality was assessed before inclusion for analysis. The gcRMA-normalized data were subjected to two-factor ANOVA for genotype (wild type and *WEE1*^{KO}) and time (0, 5, and 24 h) with The Institute for Genomic Research MultiExperiment Viewer 4.5 (TMeV 4.5; http://www.tm4.org) (*df* genotype = 1; *df* time = 2; *df* interaction = 2; and *df* error = 6) (Saeed et al., 2003). P values were based on permutations (10,000), and a multiple comparison correction was applied by calculating the false discovery rate using Mixture Model of GenStat (http://www.vsni.co.uk/software/genstat/). Genes were selected for analysis when they were 1.8-fold upregulated (≥1.8) or downregulated (≤0.56) in Col-0 or *WEE1*^{KO}, either 5 or 24 h after treatment, and if one of the three P values obtained after ANOVA analysis was <0.01 and false discovery rate < 0.1. Clustering was based on the six expression values per gene obtained by microarray analysis (Col-0 and *WEE1*^{KO} after 0, 5, or 24 h under stress conditions). After mean normalization, significant genes were clustered into seven clusters via K-means clustering; distance metric is Euclidean distance (Soukas et al., 2000). This method divides the genes in a specified number of clusters, determined in advance by calculating a figure of merit that estimates the predictive power of a certain algorithm, such as K-means clustering (Yeung et al., 2001). Finally, gene clusters were analyzed for an enrichment in genes with a certain GO annotation with BiNGO (http://www.psb.ugent.be/cbd/papers/BiNGO/Home.html) with significance level at P value < 0.01 (Maere et al., 2005).

RNA Extraction, Nanostring nCounter Assay, and Quantitative RT-PCR

RNA extraction, nCounter assay (Nanostring Technologies), and synchronization were done as described (Cools et al., 2010). Briefly, synchronized root tips were harvested and RNA was extracted from these tissues with RNeasy plant mini kit (Qiagen). RNA levels were measured with the nCounter analysis system by the VIB MicroArrays Facility (www.microarrays.be) as described (Geiss et al., 2008) or with quantitative real-time PCR (qRT-PCR) and normalized with three reference genes (*EMB2386*, *RPS26C*, and *PAC1*). RNA levels were rescaled to the levels of wild-type plants growing for 0 h on 2 mM HU. For qRT-PCR, cDNA was prepared from 1 μg of total RNA with the iScript cDNA synthesis kit (Bio-Rad) according to the manufacturer's instructions. qRT-PCR was performed with LightCycler 480 SYBR Green I Master (Roche) in a final volume of 5 μL and 0.2 mM primer concentration and analyzed with a LightCycler 480 (Roche). For each reaction, three technical repeats and four biological repeats were done. The primer sequences were 5′-TCCGGTGGAGTGGTGTAAGCAT-3′ and 5′-GGCTTCGTCACTGGCTCCTTTT-3′ for *CESA4* (AT5G44030), 5′-GCTCGCTGGTCTCGACACAAAT-3′ and 5′-GAAGTGACGTCGGAGGGATCAA-3′ for *IRX1* (AT4G18780), 5′-GGAACGTCGAGCCATGAAGAGA-3′ and 5′-GGCCGAGGAAGACTTGGATCAT-3′ for *IRX3* (AT5G17420), 5′-GATACACGCCGGAGCATTTGAC-3′ and 5′-GCACCTTCTCCTCCACGCTTTT-3′ for *XCP1* (AT4G35350), 5′-GTTTGCGGATTTGAGCCATGAGG-3′ and 5′-AACTTCCGCCACAGCTCCTTTC-3′ for *XCP2* (AT1G20850), 5′-CTCTCGTTCCAGAGCTCGCAAAA-3′ and 5′-AAGAACACGCATCCTACGCATCC-3′ for *EMB2386* (AT1G02780), 5′-TCTCTTTGCAGGATGGGACAAGC-3′ and 5′-AGACTGAGCCGCCTGATTGTTTG-3′ for *PAC1* (AT3G22110), and 5′-GACTTTCAAGCGCAGGAATGGTG-3′ and 5′-CCTTGTCCTTGGGGCAACACTTT-3′ for *RPS26C* (AT3G56340).

Microscopy Analysis

Plants used for confocal microscopy were analyzed with either LSM 510 or LSM 5 exciter confocal microscope (Zeiss). Plants were stained for 2 min in a 10 μM PI solution (Sigma-Aldrich). For GUS staining, whole seedlings were stained in a 6-well multiwell plate (Falcon 3046; Becton Dickinson) as described (Beeckman and Engler, 1994). All light microscopy samples, irrespective of whether they were stained with GUS, were cleared with lactic acid and visualized by differential interference contrast microscopes DM LB (Leica) and BX51 (Olympus).

Sorting of GFP-Positive Nuclei

P$_{WEE1}$:GFP-WEE1 plants (in a *wee1-1*) background were treated for 24 h on 10 mM HU. Root tips (400) were harvested and used for protoplasting and sorting as described (Birnbaum et al., 2003). Afterward, 200 μL of Cystain UV Precise P nuclei extraction buffer (Partec) and 800 μL of Cystain UV Precise P staining buffer (Partec) were added to the untreated and treated root tip cells (sorted and unsorted). Flow cytometry was executed with a Cyflow flow cytometer (Partec).

Comet Assay

DNA damage was detected with a CometAssay kit (Trevigen). Whole roots, harvested from plants transferred to 1 mM HU for 24 h, were prepared as described (Wang and Liu, 2006).

Accession Numbers

Microarray results have been submitted to Miamexpress (www.ebi.ac.uk/miamexpress) with accession numbers E-MEXP-3048 (−HU) and E-MEXP-3053 (+HU). Sequence data from this article can be found in the Arabidopsis Genome Initiative or GenBank/EMBL databases under the following accession numbers: WEE1, At1g02970; ATR, At5g40820; ATM, At3g48190; VND7, At1g71930; EMB2386, At1g02780; PAC1, At3g22110; and RPS26C, At3g56340.

Supplemental Data

The following materials are available in the online version of this article.

Supplemental Figure 1. Delayed Progression through Cell Cycle and G2/M in *WEE1^{KO}*.

Supplemental Figure 2. Lack of Significant DNA Damage Phenotypes after Treatment with HU in *WEE1^{KO}* Plants.

Supplemental Figure 3. Induction of Tracheary Element Differentiation Genes in *WEE1^{KO}* Root Tips upon Replication Stress.

Supplemental Figure 4. Reduced Vascular Cell Death Phenotype by Benzyladenine in *WEE1^{KO}*.

Supplemental Table 1. Transcriptional Induction in γ-Irradiated Seedlings of Genes in Cluster A (DNA Damage Genes).

Supplemental Table 2. Cell Cycle Regulation of Genes Grouped into Cluster D after Microarray Analysis.

Supplemental Data Set 1. Overview of the Seven Different Clusters with Significantly Altered Genes after Microarray Analysis.

ACKNOWLEDGMENTS

We thank the members of the cell cycle group (VIB) for fruitful discussions and useful suggestions, Jacob Pollier for help with cDNA-amplified fragment length polymorphism analysis, Frederik Coppens and Marnik Vuylsteke for help with statistical analysis, Taku Demura for *VND7pro:GUS* plants, and Martine De Cock for help in preparing the manuscript. This work was supported by grants of the Interuniversity Poles of Attraction (IUAP VI/.33) initiated by the Belgian State, Science Policy Office. T.C. is grateful to the Agency for Innovation by Science and Technology in Flanders for a predoctoral fellowship.

Received December 24, 2010; revised March 22, 2011; accepted March 30, 2011; published April 15, 2011.

REFERENCES

Alvino, G.M., Collingwood, D., Murphy, J.M., Delrow, J., Brewer, B.J., and Raghuraman, M.K. (2007). Replication in hydroxyurea: It's a matter of time. Mol. Cell. Biol. **27:** 6396–6406.

Beeckman, T., and Engler, G. (1994). An easy technique for the clearing of histochemically stained plant tissue. Plant Mol. Biol. Rep. **12:** 37–42.

Birnbaum, K., Shasha, D.E., Wang, J.Y., Jung, J.W., Lambert, G.M., Galbraith, D.W., and Benfey, P.N. (2003). A gene expression map of the *Arabidopsis* root. Science **302:** 1956–1960.

Boudolf, V., Barrôco, R., de Almeida Engler, J., Verkest, A., Beeckman, T., Naudts, M., Inzé, D., and De Veylder, L. (2004). B1-type cyclin-dependent kinases are essential for the formation of stomatal complexes in *Arabidopsis thaliana*. Plant Cell **16:** 945–955.

Boudolf, V., Inzé, D., and De Veylder, L. (2006). What if higher plants lack a CDC25 phosphatase? Trends Plant Sci. **11:** 474–479.

Branzei, D., and Foiani, M. (2010). Maintaining genome stability at the replication fork. Nat. Rev. Mol. Cell Biol. **11:** 208–219.

Churchman, M.L., et al. (2006). SIAMESE, a plant-specific cell cycle regulator, controls endoreplication onset in *Arabidopsis thaliana*. Plant Cell **18:** 3145–3157.

Clough, S.J., and Bent, A.F. (1998). Floral dip: A simplified method for *Agrobacterium*-mediated transformation of *Arabidopsis thaliana*. Plant J. **16:** 735–743.

Cook, J.G. (2009). Replication licensing and the DNA damage checkpoint. Front. Biosci. **14:** 5013–5030.

Cools, T., and De Veylder, L. (2009). DNA stress checkpoint control and plant development. Curr. Opin. Plant Biol. **12:** 23–28.

Cools, T., Iantcheva, A., Maes, S., Van Den Daele, H., and De Veylder, L. (2010). A replication stress-induced synchronization method for *Arabidopsis thaliana* root meristems. Plant J. **64:** 705–714.

Culligan, K., Tissier, A., and Britt, A. (2004). ATR regulates a G2-phase cell-cycle checkpoint in *Arabidopsis thaliana*. Plant Cell **16:** 1091–1104.

Culligan, K.M., Robertson, C.E., Foreman, J., Doerner, P., and Britt, A.B. (2006). ATR and ATM play both distinct and additive roles in response to ionizing radiation. Plant J. **48:** 947–961.

Curtis, M.J., and Hays, J.B. (2007). Tolerance of dividing cells to replication stress in UVB-irradiated Arabidopsis roots: Requirements for DNA translesion polymerases η and ζ. DNA Repair (Amst.) **6:** 1341–1358.

De Schutter, K., Joubès, J., Cools, T., Verkest, A., Corellou, F., Babiychuk, E., Van Der Schueren, E., Beeckman, T., Kushnir, S., Inzé, D., and De Veylder, L. (2007). *Arabidopsis* WEE1 kinase controls cell cycle arrest in response to activation of the DNA integrity checkpoint. Plant Cell **19:** 211–225.

De Veylder, L., Beeckman, T., Beemster, G.T.S., Krols, L., Terras, F., Landrieu, I., Van Der Schueren, E., Maes, S., Naudts, M., and Inzé, D. (2001). Functional analysis of cyclin-dependent kinase inhibitors of Arabidopsis. Plant Cell **13:** 1653–1667.

Dissmeyer, N., Weimer, A.K., De Veylder, L., Novak, B., and Schnittger, A. (2010). The regulatory network of cell cycle progression is fundamentally different in plants versus yeast or metazoans. Plant Signal. Behav. **5:** 1613–1618.

Dissmeyer, N., Weimer, A.K., Pusch, S., De Schutter, K., Lessa Alvim Kamei, C., Nowack, M.K., Novak, B., Duan, G.-L., Zhu, Y.-G., De Veylder, L., and Schnittger, A. (2009). Control of cell proliferation, organ growth, and DNA damage response operate independently of dephosphorylation of the *Arabidopsis* Cdk1 homolog CDKA;1. Plant Cell **21:** 3641–3654.

Doonan, J.H., and Sablowski, R. (2010). Walls around tumours–Why plants do not develop cancer. Nat. Rev. Cancer **10:** 794–802.

Fulcher, N., and Sablowski, R. (2009). Hypersensitivity to DNA damage in plant stem cell niches. Proc. Natl. Acad. Sci. USA **106:** 20984–20988.

Furukawa, T., Curtis, M.J., Tominey, C.M., Duong, Y.H., Wilcox, B.W. L., Aggoune, D., Hays, J.B., and Britt, A.B. (2010). A shared DNA-damage-response pathway for induction of stem-cell death by UVB and by gamma irradiation. DNA Repair (Amst.) **9:** 940–948.

Garcia, V., Bruchet, H., Camescasse, D., Granier, F., Bouchez, D., and Tissier, A. (2003). *AtATM* is essential for meiosis and the somatic response to DNA damage in plants. Plant Cell **15:** 119–132.

Geiss, G.K., et al. (2008). Direct multiplexed measurement of gene expression with color-coded probe pairs. Nat. Biotechnol. **26:** 317–325. Erratum. Nat. Biotechnol. **26,** 709.

Gould, K.L., Moreno, S., Tonks, N.K., and Nurse, P. (1990). Complementation of the mitotic activator p80^{cdc25}, by a human protein-tyrosine phosphatase. Science **250:** 1573–1576.

Harashima, H., and Schnittger, A. (2010). The integration of cell division, growth and differentiation. Curr. Opin. Plant Biol. **13:** 66–74.

Harper, J.W., and Elledge, S.J. (2007). The DNA damage response: Ten years after. Mol. Cell **28:** 739–745.

Hennig, L., Menges, M., Murray, J.A.H., and Gruissem, W. (2003). *Arabidopsis* transcript profiling on Affymetrix GeneChip arrays. Plant Mol. Biol. **53:** 457–465.

Ivanov, R., Tiedemann, J., Czihal, A., Schallau, A., Diep le, H., Mock, H.P., Claus, B., Tewes, A., and Baumlein, H. (2008). EFFECTOR OF TRANSCRIPTION2 is involved in xylem differentiation and includes a functional DNA single strand cutting domain. Dev. Biol. **313:** 93–106.

Karimi, M., De Meyer, B., and Hilson, P. (2005). Modular cloning in plant cells. Trends Plant Sci. **10:** 103–105.

Kawamoto, K., Chen, G.-X., Mano, J., and Asada, K. (1994). Photoinactivation of photosystem II by in situ-photoproduced hydroxyurea radicals. Biochemistry **33:** 10487–10493.

Kubo, M., Udagawa, M., Nishikubo, N., Horiguchi, G., Yamaguchi, M., Ito, J., Mimura, T., Fukuda, H., and Demura, T. (2005). Transcription switches for protoxylem and metaxylem vessel formation. Genes Dev. **19:** 1855–1860.

Lopes, M., Cotta-Ramusino, C., Liberi, G., and Foiani, M. (2003). Branch migrating sister chromatid junctions form at replication origins through Rad51/Rad52-independent mechanisms. Mol. Cell **12:** 1499–1510.

Lopes, M., Cotta-Ramusino, C., Pellicioli, A., Liberi, G., Plevani, P., Muzi-Falconi, M., Newlon, C.S., and Foiani, M. (2001). The DNA replication checkpoint response stabilizes stalled replication forks. Nature **412:** 557–561.

Maere, S., Heymans, K., and Kuiper, M. (2005). *BiNGO*: A Cytoscape plugin to assess overrepresentation of Gene Ontology categories in biological networks. Bioinformatics **21:** 3448–3449.

Mähönen, A.P., Bishopp, A., Higuchi, M., Nieminen, K.M., Kinoshita, K., Törmäkangas, K., Ikeda, Y., Oka, A., Kakimoto, T., and Helariutta, Y. (2006). Cytokinin signaling and its inhibitor AHP6 regulate cell fate during vascular development. Science **311:** 94–98.

Menges, M., Hennig, L., Gruissem, W., and Murray, J.A.H. (2003). Genome-wide gene expression in an *Arabidopsis* cell suspension. Plant Mol. Biol. **53:** 423–442.

Mourelatou, M., Doonan, J.H., and McCann, M.C. (2004). Transition of G1 to early S phase may be required for zinnia mesophyll cells to trans-differentiate to tracheary elements. Planta **220:** 172–176.

Peres, A., et al. (2007). Novel plant-specific cyclin-dependent kinase inhibitors induced by biotic and abiotic stresses. J. Biol. Chem. **282:** 25588–25596.

Perry, J.A., and Kornbluth, S. (2007). Cdc25 and Wee1: Analogous opposites? Cell Div. **2:** 12.

Porceddu, A., Stals, H., Reichheld, J.-P., Segers, G., De Veylder, L., De Pinho Barrôco, R., Casteels, P., Van Montagu, M., Inzé, D., and Mironov, V. (2001). A plant-specific cyclin-dependent kinase is involved in the control of G_2/M progression in plants. J. Biol. Chem. **276:** 36354–36360.

Postow, L., Ullsperger, C., Keller, R.W., Bustamante, C., Vologodskii, A.V., and Cozzarelli, N.R. (2001). Positive torsional strain causes the formation of a four-way junction at replication forks. J. Biol. Chem. **276:** 2790–2796.

Preuss, S.B., and Britt, A.B. (2003). A DNA-damage-induced cell cycle checkpoint in Arabidopsis. Genetics **164:** 323–334.

Ricaud, L., Proux, C., Renou, J.P., Pichon, O., Fochesato, S., Ortet, P., and Montane, M.H. (2007). ATM-mediated transcriptional and developmental responses to gamma-rays in Arabidopsis. PLoS ONE **2:** e430.

Riha, K., Watson, J.M., Parkey, J., and Shippen, D.E. (2002). Telomere length deregulation and enhanced sensitivity to genotoxic stress in *Arabidopsis* mutants deficient in Ku70. EMBO J. **21:** 2819–2826.

Saban, N., and Bujak, M. (2009). Hydroxyurea and hydroxamic acid derivatives as antitumor drugs. Cancer Chemother. Pharmacol. **64:** 213–221.

Saeed, A.I., et al. (2003). TM4: A free, open-source system for microarray data management and analysis. Biotechniques **34:** 374–378.

Segurado, M., and Tercero, J.A. (2009). The S-phase checkpoint: Targeting the replication fork. Biol. Cell **101:** 617–627.

Sogo, J.M., Lopes, M., and Foiani, M. (2002). Fork reversal and ssDNA accumulation at stalled replication forks owing to checkpoint defects. Science **297:** 599–602.

Sørensen, C.S., Syljuåsen, R.G., Falck, J., Schroeder, T., Rönnstrand, L., Khanna, K.K., Zhou, B.-B., Bartek, J., and Lukas, J. (2003). Chk1 regulates the S phase checkpoint by coupling the physiological turnover and ionizing radiation-induced accelerated proteolysis of Cdc25A. Cancer Cell **3:** 247–258.

Soukas, A., Cohen, P., Socci, N.D., and Friedman, J.M. (2000). Leptin-specific patterns of gene expression in white adipose tissue. Genes Dev. **14:** 963–980.

Swoboda, P., Gal, S., Hohn, B., and Puchta, H. (1994). Intrachromosomal homologous recombination in whole plants. EMBO J. **13:** 484–489.

Turner, S., Gallois, P., and Brown, D. (2007). Tracheary element differentiation. Annu. Rev. Plant Biol. **58:** 407–433.

Wang, C., and Liu, Z. (2006). *Arabidopsis* ribonucleotide reductases are critical for cell cycle progression, DNA damage repair, and plant development. Plant Cell **18:** 350–365.

Willis, N., and Rhind, N. (2009). Regulation of DNA replication by the S-phase DNA damage checkpoint. Cell Div. **4:** 13.

Yamaguchi, M., Goué, N., Igarashi, H., Ohtani, M., Nakano, Y., Mortimer, J.C., Nishikubo, N., Kubo, M., Katayama, Y., Kakegawa, K., Dupree, P., and Demura, T. (2010). VASCULAR-RELATED NAC-DOMAIN6 and VASCULAR-RELATED NAC-DOMAIN7 effectively induce transdifferentiation into xylem vessel elements under control of an induction system. Plant Physiol. **153:** 906–914.

Yamaguchi, M., Kubo, M., Fukuda, H., and Demura, T. (2008). VASCULAR-RELATED NAC-DOMAIN7 is involved in the differentiation of all types of xylem vessels in Arabidopsis roots and shoots. Plant J. **55:** 652–664.

Yeung, K.Y., Haynor, D.R., and Ruzzo, W.L. (2001). Validating clustering for gene expression data. Bioinformatics **17:** 309–318.

Yoshiyama, K., Conklin, P.A., Huefner, N.D., and Britt, A.B. (2009). Suppressor of gamma response 1 (*SOG1*) encodes a putative transcription factor governing multiple responses to DNA damage. Proc. Natl. Acad. Sci. USA **106:** 12843–12848.

Zegerman, P., and Diffley, J.F.X. (2009). DNA replication as a target of the DNA damage checkpoint. DNA Repair (Amst.) **8:** 1077–1088.

Zhao, H., Watkins, J.L., and Piwnica-Worms, H. (2002). Disruption of the checkpoint kinase 1/cell division cycle 25A pathway abrogates ionizing radiation-induced S and G_2 checkpoints. Proc. Natl. Acad. Sci. USA **99:** 14795–14800.